Experimental study of the aqueous phase reaction of hydrogen sulfide with MEA-triazine using in situ Raman spectroscopy

Romero Logrono, Iveth Alexandra; Kucheryavskiy, Sergey; Maschietti, Marco

Published in:
Industrial & Engineering Chemistry Research

DOI (link to publication from Publisher):
10.1021/acs.iecr.1c03833

Publication date:
2021

Document Version
Accepted author manuscript, peer reviewed version

Experimental study of the aqueous phase reaction of hydrogen sulfide with MEA-triazine using in situ Raman spectroscopy

*Iveth Romero, Sergey Kucheryavskiy, Marco Maschietti**

Department of Chemistry and Bioscience, Aalborg University Esbjerg, Niels Bohrs Vej 8, 6700, Esbjerg, Denmark

*Corresponding author (e-mail: marco@bio.aau.dk)

Abstract

A method for quantitation of bisulfide in the aqueous phase reactions of H_2S scavenging with MEA-triazine is proposed. The method is based on time resolved in situ Raman spectroscopy, thus allowing in situ monitoring of the reactions. The method has been applied to obtain kinetic data of the reactions in batch configuration at room temperature for initial pH values 9, 10 and 11 and MEA-triazine/bisulfide initial concentration ratios in the range of 0.5 to 10. The pH increases remarkably during the reactions, causing a substantial decrease in the rate of disappearance of bisulfide. If the system is re-acidified, complete depletion of bisulfide can be achieved, evidencing the irreversibility of the scavenging reactions. The results are also supported by a qualitative analysis of the trends of the characteristic Raman peaks of MEA-triazine, dithiazine and monoethanolamine. These trends are in line with the currently accepted reaction scheme, consisting of two scavenging reactions in series.

1. Introduction

Hydrogen sulfide (H_2S) is a sour gas that is naturally encountered in exploration and production of hydrocarbons. It is highly corrosive to metals and poses a serious health and environmental threat because of its high toxicity. Its concentration in export oil and gas streams must be within allowable limits, which often requires its removal from the produced fluids at the oil and gas separation facilities near the wellheads.[1] With regard to natural gas, the export specifications typically require a maximum concentration below 4 ppm.[2]

One of the methods available for the removal of H_2S from natural gas streams is the direct injection of H_2S scavengers, which are chemicals reacting with H_2S and transforming it into substantially less toxic and corrosive species.[2] The applicability of H_2S scavenging is limited to H_2S concentrations in the gas typically up to approximately 5000 ppmv due to the process economics.[1] The most common H_2S scavengers used nowadays are 1,3,5-hexahydrotriazines, often simply called triazines, with 1,3,5-tris(2-hydroxyethyl)-hexahydro-s-triazine (HET) being largely predominant (at least 80% of the oilfield market[3]) due to its high scavenging efficiency, high solubility in water, as well as a high solubility in water of its byproducts.[2,4] In particular, the injection of HET into gas streams is the preferred H_2S scavenging method in topside process units in offshore oil and gas production due to the low footprint and simplicity of implementation. The process consists in injecting and dispersing a basic aqueous solution of HET in the wet gas, inducing the absorption of H_2S in the dispersed liquid phase where the scavenging reaction actually takes place, thus enhancing the absorption itself.

To date, it is accepted that the aqueous phase reaction of H_2S with HET occurs through a multiple reaction scheme, which is reported in simplified form in Figure 1. The first step involves the protonation of HET and its reaction with HS^- producing 3,5-bis(2-hydroxyethyl)hexahydro-1,3,5-thiadiazine

(thiadiazine, TDZ) and monoethanolamine (MEA). TDZ, in turn, can also undergo protonation and reaction with HS^- leading to 5-(2-hydroxyethyl)hexahydro-1,3,5-dithiazine (dithiazine, DTZ) and another molecule of MEA. The substitution of a third sulfur atom into the triazine ring, which would give trithiane, is instead typically not observed.[1,5-12] This is presumably attributed to the absence of a nucleophilic carbon center in DTZ susceptible of an attack by HS^-, as opposed to TDZ.[1] Thus, from a stoichiometric standpoint, two moles of sulfur from H_2S can be converted into DTZ by using one mole of HET, with the liberation of two moles of MEA. The production of MEA in the scavenging reaction with HET is the reason for the common name of this scavenger in the oil and gas industry, where it is typically referred to as MEA-triazine.

Typical field values of injection of triazine-based commercial scavengers (aqueous solutions 40-50 wt.%) are in the range of 12 to 20 kg of commercial product for the removal of 1 kg of H_2S.[2] The stoichiometric requirement that can be calculated from the abovementioned stoichiometry gives 6 to 8 kg of commercial MEA-triazine based scavenger per 1 kg of H_2S. Thus, a large stoichiometric excess of HET is actually used by offshore oil and gas operators, which is detrimental to the environment, due to the discharge of relatively large amounts of unspent scavenger into the sea, and to the operating expenditures, since a large part of the injected HET is actually not reacting with H_2S.[13] The application of a large excess of MEA-triazine is a conservative measure owing to insufficient fundamental physicochemical knowledge of the absorption-reaction process and consequent lack of predictability of the outcome of the operation as a function of the design variables (e.g. injector type, gas velocity, temperature, partial pressures).[2,14] The lack of experimental quantitative data on the rate of the H_2S scavenging reaction with HET is one of the factors hindering the development of physicochemical models of the absorption-reaction process, which could allow a rational design of this operation.

To the best of our knowledge, quantitative experimental data on the rate of the aqueous phase reaction of HS^- with HET have not been reported in the literature, except for the work of Bakke and Buhaug.[6] However, in their work the authors focused on operating conditions under excess of HS^-, which are unrealistic in field operation due to the employed excess of HET and to the concurrence of the H_2S absorption and its reaction with HET in the aqueous phase. It is noted that the authors alleged that their attempts in measuring the concentration of HS^- by means of a sulfide-sensitive electrode failed to provide reproducible results. Their kinetic study was thus focused on the variation of the HET concentration over time under excess of HS^- with the reaction observed to be of first order with respect to HET.

A few studies recently reported in the literature proposed the use of Raman spectroscopy as a tool for monitoring H_2S scavenging reactions with HET.[15-17] More specifically, Perez-Pineiro et al.[16] reported the use of Raman spectroscopy for quantitation of HET and DTZ in spent scavenger samples. Furthermore, OndaVia has made available cartridges and instrumentation for the assay of HET and DTZ by Raman spectroscopy.[18] In a previous work from our research group,[17] it was shown that it is possible to online monitor the decrease of HS^- over time in the scavenging reaction with HET and to detect the appearance of the characteristic Raman bands associated with the carbon-sulfur bonds of the reaction products. However, no internal standard was used, which made the results merely qualitative. The reaction rate was however observed to depend strongly on the pH.

The objective of this work is two-fold: (i) to develop a method for in situ accurate quantitative measurement of the HS^- concentration during the aqueous phase reaction between HET and HS^- based on Raman spectroscopy and chemometrics methods for spectral pre-processing and analysis; and (ii) to generate novel experimental data for the rate of disappearance of HS^- in the aqueous phase scavenging reactions with HET under relevant conditions for industrial applications (i.e. excess of HET). The study is based on batch-reaction experiments carried out at room temperature for three different values of the

initial pH (9, 10 and 11) and four different HET to HS^- initial concentration ratios (in the range of 0.5 to 10). In addition, the methodology allows a qualitative analysis of the development of the main scavenging reaction products over time.

2. Materials and Methods

2.1. Materials

Aqueous solutions of 1,3,5-tris(2-hydroxyethyl)hexahydro-s-triazine (HET; CAS 4719-04-4) of technical purity, hereinafter termed technical triazine solution, were used as H_2S scavenger. Monoethanolamine (MEA) is the main impurity of this solution. The concentration of HET and MEA was determined by means of GC-FID analysis, according to a method reported elsewhere,[13] and was found to be 2.60 M ± 0.06 M and 2.06 M ± 0.39 M, respectively. The density of the triazine solution was measured by weighing accurately measured volumes of the solution by means of an analytical balance (Sartorious 1702, accuracy 0.1 mg). The volumes were measured by means of a precision pipette (Finn F2, 0.5 – 5 mL, Thermo Scientific, accuracy 0.03 mL) previously calibrated with distilled water at 20°C. Measurements were done in quintuplicate. The density of the triazine solution at 20 °C resulted in being 1.11 g/mL ± 0.01 g/mL. The pH of the solution was 10.9. All pH values reported in this work were measured with a pH meter (Metrohm, 914 pH/conductometer) and a microelectrode (Metrohm, 6.0234.110) calibrated prior to the execution of each experimental run with a two-point calibration between pH 7.0 and 10.0 at 22 °C.

Disodium sulfide about trihydrate ($Na_2S\cdot\sim3H_2O$; CAS 27610-45-3) from VWR Chemicals (product ID 83756.230) was used to prepare aqueous bisulfide solutions that were used both as reactant and as standard solutions for the determination of Raman calibration curves. The declared impurities in the

product, on a water-free basis, are limited to nitrogen (max. 0.0125 wt.%), sulfur trioxide (SO_3, max. 0.6 wt.%) and thiosulfate (S_2O_3, max. 0.5 wt.%). The actual degree of hydration of sodium sulfide (grams of water per grams of wet solid) used for preparing the samples was measured by means of Karl Fischer (KF) titration (870 KF Titrino plus, Metrohm AG), equipped with an oven (860 KF Thermoprep, Metrohm AG) where the sample was thermally prepared at 210 °C. KF titrations were carried out in triplicate. The degree of hydration was found to be 38.2 wt.% with a relative standard deviation (RSD) equal to 1.79%.

Aqueous solutions of hydrochloric acid (HCl) 6 M were used for pH adjustment and prepared from fuming hydrochloric acid from Merck Chemicals (product ID 1.00317, HCl ≥ 37 wt.%). MEA from Sigma-Aldrich (product ID 02400, purity ≥ 99 wt.%), HET from Santa Cruz Biotechnology (CAS 4719-04-4; product ID sc-474806; purity ≥ 95 wt.%) and DTZ (CAS 88891-55-8; product ID D493850, purity > 98 wt.%) from Toronto Research Chemicals were used as analytical standards. Analytical grade acetonitrile from VWR Chemicals (product ID 83640.290, purity ≥ 99.9 wt.%) was used as internal standard (IS) for calibration and determination of HS^- concentrations in the reaction experiments.

The aqueous solutions of reactants used in the present work were prepared with distilled water previously stripped with nitrogen for removal of dissolved oxygen to a final concentration between 0.01 and 0.02 mg/L at 22 °C, measured with a portable oxygen meter (OxyGuard, Handy Polaris 2, measuring range 0 – 60 ppm, 0 – 600 % saturation).

2.2. Reaction experiments

All experiments were carried out in batch mode at room temperature (21-22 °C) with an initial concentration of HS^- of 100 mM. One experimental campaign was based on a full factorial design with

two factors: the initial concentration of HET (three levels: 100 mM, 500 mM, and 1000 mM) and the initial pH (pH_0, three levels: 9, 10 and 11). For each combination, two solutions were prepared independently, which resulted in 18 reaction runs. All runs were carried out in a randomized order. Each reaction was monitored for three hours. Subsequently, the aqueous reacting phase was acidified back to a value as close as possible to pH_0 and then monitored for three additional hours, in order to allow verifying the possibility of completing the reaction.

The experimental data provided by Bakke et al.[5] indicate that the hydrolysis of HET at high pH values is slow enough to be neglected. The actual pH established in the aqueous phase in contact with the sour gas stream in field operational use depends on the balancing between the H_2S absorption, which tends to decrease the pH of the aqueous phase, and the scavenging reactions, which tend to increase it. Technical solutions of HET have a pH around 11 (see Section 2.1), while spent scavenger samples are seen with a pH around 9.[13] The pH of the aqueous phase in contact with the sour gas is expected to be in the range of 8-9 to 11-12. Based on the rate constants determined by Bakke et al.,[5] the expected loss of HET due to hydrolysis in our experiments should not be above 0.22%. Therefore, the initial pH values applied in this work allow neglecting the hydrolysis of HET as a side reaction. In addition, the re-acidifications allowed restoring pH values within the ranges of interest in field operation, while re-starting the reactions in the presence of unconverted bisulfide and HET and therefore acquiring additional experimental data.

A second experimental campaign was carried out with an initial concentration of HET of 50 mM, at three levels of pH_0: 9, 10 and 11. Also in this case, experiments for each combination of the two factors were carried out in duplicate with independent preparation of the solutions charged to the reactor. This experimental campaign was planned after analyzing the data of the first experimental campaign with the aim of analyzing the reacting system at high fractional conversions of HET and high yields of DTZ. In all the experiments of the second campaign, the reacting system was monitored for a total time of 6 hours

and acidified back to values close to pH_0 three times (after 3.0 h, 4.0 h and 5.0 h). In total, 24 reaction experiments were carried out in the two campaigns.

With regards to the execution of the reactions, a certain mass of the technical triazine solution (1.07 g, 2.13 g, 10.65 g or 21.31 g) was diluted in distilled water, conditioned to the desired pH_0, and brought to 25 mL with further addition of distilled water using a class A volumetric flask. A certain mass of $Na_2S \cdot \sim 3H_2O$ (ca. 0.64 g), whose degree of hydration was preliminarily measured, was dissolved in distilled water, mixed with a certain amount of IS (ca. 0.21 g), pH-adjusted to the desired value and brought to 25 mL with further addition of distilled water using a class A volumetric flask. The initial pH values of the two solutions were 9, 10 or 11. Two 10-mL aliquots of the solutions of HS^- + IS and HET were withdrawn by means of glass volumetric pipettes (class A, 10 mL ± 0.02 mL) mixed in a Raman glass vial closed with a threaded lid and placed inside a dark camera for in situ monitoring of the scavenging reactions. The time elapsed from the start of the mixing of the reagent solutions (reaction time zero) to the start of the spectral acquisition was in the range of 18 to 25 seconds.

After 3 hours of monitoring time, the pH of the reacting system was measured. The pH was found to increase in all cases. Then, the system was re-acidified following the abovementioned procedure. For all cases, the time elapsed from the end of a stage of the reaction (i.e. prior to a re-acidification) to the start of a new spectral acquisition (i.e. after the re-acidification) was in the range of 2 to 5 minutes.

2.3. Raman spectroscopy and data analysis

The quantitation of aqueous solutions containing HS^- was carried out by Raman spectroscopy (Rxn1-785, Kaiser Optical Systems) using a 785-nm laser as the source of excitation light with a non-contact probe. The solutions were put into a glass vial suitable for Raman spectroscopy analyses (capacity 20 mL) placed inside a dark camera to avoid the entrance of external light into the system. The spectra were

177 taken by the probe located around 1 cm from the vial. For each acquisition, three consequent spectra
178 were taken using 5 seconds excitation time and averaged to increase the signal to noise ratio.

179 In order to measure the concentration of HS^-, a Partial Least Squares regression (PLSR)[19] model was
180 calibrated. The calibration was based on Raman spectra acquired for solutions containing 100 mM of
181 internal standard (IS) and HS^- concentration varying in the range of 10 mM to 100 mM (10 concentration
182 levels in total with equal step size). The pH of the solutions was set to 9.0 ± 0.2. Each standard solution
183 was prepared independently and in triplicate giving 30 samples in total.

184 In order to make the regression model robust, the spectra were preprocessed and truncated before the
185 calibration. The best results were achieved by using a two-step preprocessing procedure: baseline
186 correction using alternating least squares method[20] with lambda equal to 10^5 and a penalty of 0.025 and
187 normalization of the corrected spectra to the sum of intensities between wave numbers 2255 cm^{-1} and
188 2265 cm^{-1}, corresponding to the area around the IS peak. After that, the spectra were truncated around
189 the characteristic Raman shift for HS^- identified at 2575 cm^{-1} (2565–2581 cm^{-1}). The preprocessed and
190 truncated spectra used for calibration of the PLSR model are shown in the left part of Figure 2. The color
191 gradient is utilized to illustrate the concentration of HS^- in the solution, for which the spectra were
192 acquired. Because neither the characteristic peak of HS^- nor the IS peak overlap with the Raman peaks
193 of the other reaction products, this procedure makes it possible to use the regression model also for the
194 solutions, where other chemical components are present.

195 The selection of the best preprocessing conditions was carried out based on cross-validation results
196 using PLSR models with one component. The prediction performance of the final model is characterized
197 by a coefficient of determination (R^2) equal to 0.993 and root mean squared error (RMSE) equal to 2.595
198 mM. The right part of Figure 2 demonstrates the corresponding predicted vs. measured values for HS^-
199 for cross-validated predictions.

The final model was also validated on a test set, i.e. another set of bisulfide solutions prepared using pH 9, 10, and 11. The test results showed that the prediction performance of the model calibrated using samples with pH 9 works equally well for the samples with pH 10 and 11, so the same regression model can be used for a wide range of pH values.

The developed PLSR model was then employed for online prediction of HS^- during the scavenging reactions. The in situ analysis of the reaction mixtures was performed with auto-sampling acquiring the average of 3 spectra for 5 seconds in intervals of 30 seconds. In total, 720 spectra were collected in each reaction experiment.

The data analysis and all visualizations were performed in R (v. 4.0.2)[21] using the package *mdatools*.[22] The package *hyperSpec*[23] was utilized to import spectral data from spectral files created by the spectrometer.

In addition, characteristic Raman bands were identified for HET, MEA and DTZ by analyzing the Raman spectra of analytical standards. Aqueous solutions of the analytical standards of HET (100 mM) and DTZ (20 mM) were prepared using distilled water, while analytical grade MEA was used without previous dilution. Spectra of the solutions were acquired with the same equipment and procedure described above. The spectra were slightly denoised using the Savitzky-Golay filter, normalized to a unit length and truncated to the range from 300 to 2500 cm^{-1}. Transformations and plots were performed in R using the package *mdatools*.[22]

3. Results and Discussion

3.1. Effect of HET concentration and pH on the scavenging reactions

The initial concentrations of HET, MEA, HS^- and IS, as well as the initial pH of the 12 operating conditions are available in the Supporting Information (Table S1). Besides the scavenging reactions in

223 the presence of HET, two additional experiments were carried out in order to verify the stability of the
224 Raman peaks of MEA, HS^- and IS in the absence of HET. Both experiments revealed stable intensity of
225 the Raman peaks, as shown in the Supporting Information (Figures S1-S2). All reaction samples were
226 homogeneous and transparent in all runs and at any reaction time without any sign of solid precipitation.
227 Figures 3-5 show the effect of the initial concentration of HET and of pH_0 on the conversion of HS^-. The
228 vertical dashed lines correspond to the acidification of the reacting system back to the initial pH carried
229 out after 3 hours. The dotted lines correspond to the additional re-acidifications, which were carried out
230 in the runs with the initial concentration of HET of 50 mM only (see Section 2.2). The plot also reports
231 the values of pH after 3 hours (just before the first acidification) and the pH values after 6 hours. The
232 figures refer to one of the two duplicates, for ease of visualization. The duplicates show the same features
233 and match very well with ARD values in the first three hours (prior to acidification) in the range of 3.1%
234 to 10.4% for the 12 operating conditions, being 5.3% on average. After the first three hours of reaction,
235 qualitatively reproducible trends were observed for all executions. The complete set of figures, together
236 with ARD values for each duplicate execution, is reported in Figures S3-S5 and Table S2 of the
237 Supporting Information.
238 As can be seen from Figures 3-5, the decrease in the reaction rate is very pronounced, as the time
239 increases, with the concentration of HS^- appearing not to reduce to zero. Concurrently, the pH of the
240 reacting system largely increases during the reaction, reaching values above 11.8 for all runs. The
241 increase of pH is in line with the reaction mechanism involving the protonation of HET and TDZ, as
242 reported in Section 1. In fact, the consumption of HET and TDZ cations due to the scavenging reactions
243 induces new HET and TDZ molecules to be protonated according to the Le Chatelier's principle, thus
244 consuming H_3O^+ and raising the pH of the solution. In turn, higher pH values reduce the fraction of HET
245 and TDZ existing in protonated form, as typical pK_a values of amines are in the range 7 to 11,[24] thus

246 reducing the availability of HET and TDZ cations and inhibiting the scavenging reactions themselves.
247 The effect is particularly visible at the lowest initial pH (Figure 3) for the largest excess of HET (initial
248 concentration ratio of 10), where approximately 60% of the initial HS^- is converted in the first seven
249 minutes of reaction, while only additional 20% is converted by the end of 3 hours. At this point, the
250 concentration of HS^- stabilizes at values around 20 mM even in the presence of a large excess of HET
251 still available. As can be seen, the pH of the system reached values close to 12.3, at which the fraction
252 of HET and TDZ existing in protonated form must be extremely small when considering the
253 abovementioned pKa values. Additionally, in this case the acidification carried out at three hours caused
254 the swift and complete depletion of the unreacted HS^- in only approximately two minutes, clearly
255 showing that the previous reaction stop was caused by high pH and not by the reduction in the
256 concentration of HET and HS^-. The same pattern is observed for the initial concentration ratio of five.
257 The fact that HS^- can be completely depleted shows that the scavenging process is irreversible at room
258 temperature, provided that the pH is maintained at values below approximately 12. At lower HET/HS^-
259 initial concentration ratios, such an abrupt change in the rate of reaction is not observed, because the
260 reaction is slower and, therefore, the pH increase is also slower.

261 Figures 3-5 also show the effect of the excess of HET on the rate of reaction for given initial pH values.
262 The rate of conversion of HS^- is observed to increase substantially with the initial concentration of HET.
263 Bakke and Buhaug[6] proposed a first order reaction with respect to HET, with the information on the rate
264 equation derived under the assumption of constant pH attained with a 0.5 M Na_2HPO_4 buffer. We also
265 carried out the reaction in the presence of the same buffer and measured the pH of the reacting system
266 online (see Supporting Information, Figure S6); however, we observed a substantial variation of pH even
267 in the presence of such a buffer. Therefore, the kinetic determinations of Bakke and Buhaug[6] are
268 considered only qualitative. Overall, it can yet be stated that the positive correlation between the

concentration of HET and the rate of reaction is not in disagreement with the findings of Bakke and Buhaug.[6]

Table 1 shows numerical examples of the fractional conversion of HS^- at specified times. For instance, after 1 hour of reaction for $pH_0 = 9$, the fractional conversion of HS^- increases from 12% to 72% as the initial concentration of HET is increased from 50 to 1000 mM. The same trend is observed at higher initial pH values, i.e. 10 and 11, even though the maximum fractional conversions obtained for the cases with 1000 mM of HET reach 53% and 41%, respectively, due to the inhibition of high pH values. For fixed values of the initial concentration ratio HET/HS^- and reaction time, the reduction of the fractional conversion with the increase of the initial pH is clearly visible from Table 1.

3.2. Identification and monitoring of key species in the scavenging reactions

The acquired spectra of analytical standards of HET, DTZ and MEA were analyzed to identify characteristic Raman peaks to monitor qualitatively the progress of the scavenging reactions, besides the quantitative analysis of the rate of disappearance of HS^- discussed in Section 3.1. The acquired spectra are shown in Figure S7 of the Supporting Information. As a result of the analysis, the peaks used as indicators of HET, DTZ and MEA are respectively 923 cm^{-1}, 675 cm^{-1} and 840 cm^{-1}, which are consistent with the information available in the literature.[15,16,18]

Figure 6 shows the evolution of the spectra over time in one of the reaction runs for $pH_0 = 9$ and HET/HS^- initial concentration ratio of 0.5 in the period between 3 h and 6 h of reaction. The selected peaks for HET, DTZ and MEA are clearly observable in the reaction spectra. Even though the selected peak for DTZ is partially overlapping with a broad peak from HET (approximately 700 cm^{-1}), the latter is observed to be constant during the scavenging reaction. This makes it possible to associate, on a qualitative level, the variations of the peak at 675 cm^{-1} with the variations of the concentration of DTZ.

292 Noticeably is the clear decrease of the peaks of HS^- and HET and the concurrent increase of the peaks
293 of MEA and DTZ. The development of the peak at 634 cm^{-1} is also noted, which shows a maximum
294 point followed by a decrease with the advancement of the scavenging reaction suggesting to be related
295 to an intermediate product of the series of reactions. This peak may be representative of TDZ, in line
296 with the Raman band associated to TDZ by Perez-Pineiro et al.[15] Moreover, Figure 7 shows the relative
297 intensity (with respect to the height of the IS peak) of the selected peaks as a function of time and as a
298 function of the fractional conversion of HS^- (X) corresponding to reactions at $pH_0 = 9$ and four levels of
299 HET/HS^- initial concentration ratios. In all the cases, the acidification of the system at t = 3 hours causes
300 a sudden change of the intensity of the peaks of HET, DTZ and MEA, which clearly indicates how the
301 pH reduction increases the rate of the scavenging reactions. In the cases of HET/HS^- initial concentration
302 ratios of 5 and 10, i.e. large excess of HET, the sudden change is associated with swift and complete
303 depletion of HS^- (X=1), and it is therefore followed by stable signals. For an HET/HS^- initial
304 concentration ratio of 1, the sudden change is associated with a swift increase in the fractional conversion
305 of HS^-, from approximately 0.3 to 0.6, which is followed by a slow additional consumption of HET and
306 the formation of DTZ. For an HET/HS^- initial concentration ratio of 0.5, the acidification leads to a swift
307 increase in the fractional conversion of HS^-, from approximately 0.2 to 0.4. Interestingly, in this case the
308 trend of the intensity of the DTZ peak exhibits an upward concavity until approximately 5.5 hours,
309 meaning that the rate of formation of DTZ increases over time, which is observed only at these
310 conditions. This can be explained by the second scavenging reaction progressing to a larger extent,
311 compared to cases where a large excess of HET is present, where the scavenging of HS^- is mainly attained
312 by the first scavenging reaction. Regarding MEA (840 cm^{-1}), a linear increase of its peak intensity with
313 respect to the fractional conversion of HS^- is observed. This is in line with the expected formation of
314 MEA from both the first and the second scavenging reaction, with a 1:1 stoichiometric ratio with respect

315 to HS^- in both reactions. All the cases related to the trends of the selected peaks at different initial pH
316 are available in Figures S8-S22 in the Supporting Information.
317
318 **4. Conclusions**
319 We are the first to provide quantitative measurements of HS^-, the prevailing form of H_2S in basic
320 aqueous solutions of scavengers, during the aqueous phase scavenging reactions with MEA-triazine. This
321 result was accomplished by in situ acquisition of Raman spectra and the application of a PLS regression
322 model. The results confirm that the rate of the scavenging process with MEA-triazine is strongly
323 dependent on pH and that high pH values inhibit the reactions. This is in line with the currently accepted
324 reaction mechanism, which is based on the protonation of HET and TDZ followed by reaction with HS^-.
325 A remarkable dependence of the rate of disappearance of HS^- on the concentration of HET is also
326 observed with the HS^- conversion being faster at higher concentrations of HET. In addition, it is observed
327 that the buildup of DTZ is strongly dependent on the initial HET/HS^- ratio: low amounts of DTZ are
328 formed in the presence of high excess of HET, whereas a substantial buildup of DTZ can be observed
329 with stoichiometric ratio HET/ HS^- (i.e. 0.5) in the feed and long reaction times. The experimental
330 measurements and the qualitative observations of this work are expected to pave the way to the
331 development of kinetic models of the aqueous phase reactions between HS^- and HET, which are still
332 lacking in the literature.
333

334 **Supporting Information**

335 Initial concentrations and initial pH values for the two experimental campaigns and the stability tests
336 of HS^-, MEA and IS in water. Plots showing the effect of the initial concentration of HET on the

337 conversion of HS^- for duplicate executions at pH_0 = 9, 10 and 11. Average relative deviation (ARD) of
338 all the executions before the first acidification. On-line pH measurements for one reaction experiment
339 using a pH buffer solution. Raman spectra of analytical standards of HET, DTZ and MEA. Plots of the
340 intensity of the peaks at 923 cm^{-1}, 634 cm^{-1}, 675 cm^{-1} and 840 cm^{-1} for all the executions at pH_0 = 9, 10
341 and 11.

342

343 **Author information**

344 Corresponding author:

345 Marco Maschietti – Department of Chemistry and Bioscience, Aalborg University Esbjerg, Niels Bohrs
346 Vej 8, 6700, Esbjerg, Denmark; https://orcid.org/0000-0002-3120-7560; Email: marco@bio.aau.dk;

347 Authors:

348 Iveth Romero – Department of Chemistry and Bioscience, Aalborg University Esbjerg, Niels Bohrs Vej
349 8, 6700, Esbjerg, Denmark; https://orcid.org/0000-0003-1310-7889

350 Sergey Kucheryavskiy – Department of Chemistry and Bioscience, Aalborg University Esbjerg, Niels
351 Bohrs Vej 8, 6700, Esbjerg, Denmark; https://orcid.org/0000-0002-3145-7244

352 Notes

353 The authors declare no competing financial interest.

354

355 **Acknowledgements**

This work was financially supported by the Energiteknologiske Udviklings-og Demonstrationsprogram (EUDP) [Energy Technology Development and Demonstration Program], Denmark [SCAVOP project, project number 64018-0819]. The authors are grateful to Anders Andreasen (Ramboll) for the inspiring discussions on the topic in general and for his comments on the manuscript, to Rudi P. Nielsen (Aalborg University) for the inspiring discussions on technical aspects of the experimental executions, and to Susanne Tolstrup for proofreading the manuscript.

References

(1) Wylde, J. J.; Taylor, G. N.; Sorbie, K. S.; Samaniego, W. N. Formation, Chemical Characterization and Oxidative Dissolution of Amorphous Polymeric Dithiazine (Apdtz) During the Use of the H_2S Scavenger Monoethanolamine-Triazine. *Energy Fuels* **2020,** *34*, 9923-9931. https://doi.org/10.1021/acs.energyfuels.0c01402

(2) Kelland, M. Hydrogen Sulfide Scavengers, in: *Production Chemicals for the Oil and Gas Industry*; CRC Press: Boca Raton, 2014, 353-368. https://doi.org/10.1201/b16648

(3) Taylor, G.; Smith-Gonzalez, M.; Wylde, J.; Oliveira, A. H_2S Scavenger Development During the Oil and Gas Industry Search for an MEA Triazine Replacement in Hydrogen Sulfide Mitigation and Enhanced Monitoring Techniques Employed During Their Evaluation. *Proceedings in SPE International Conference on Oilfield Chemistry*, Galveston, Texas, USA, 2019, SPE-193536-MS, https://doi.org/10.2118/193536-MS

(4) Taylor, G. N.; Matherly, R. Gas Chromatography Mass Spectrometric Analysis of Chemically Derivatized Hexahydrotriazine-Based Hydrogen Sulfide Scavengers: 1. *Ind. Eng. Chem. Res.* **2010,** *49,* 5977-5980. https://doi.org/10.1021/ie100047b

(5) Bakke, J. M.; Buhaug, J.; Riha, J. Hydrolysis of 1,3,5-Tris(2-Hydroxyethyl)Hexahydro-S-Triazine and Its Reaction with H_2S. *Ind. Eng. Chem. Res.* **2001,** *40*, 6051-6054. https://doi.org/10.1021/ie010311y

(6) Bakke, J. M.; Buhaug, J. B. Hydrogen Sulfide Scavenging by 1,3,5-Triazinanes. Comparison of the Rates of Reaction. *Ind. Eng. Chem. Res.* **2004,** *43*, 1962-1965. https://doi.org/10.1021/ie030510c

(7) Taylor, G. N.; Matherly, R. Gas Chromatographic-Mass Spectrometric Analysis of Chemically Derivatized Hexahydrotriazine-Based Hydrogen Sulfide Scavengers: Part II. *Ind. Eng. Chem. Res.* **2010,** *49*, 6267-6269. https://doi.org/10.1021/ie1001247

(8) Taylor, G. N.; Matherly, R. Structural Elucidation of the Solid Byproduct from the Use of 1,3,5-Tris(Hydroxyalkyl)Hexahydro-*S*-Triazine Based Hydrogen Sulfide Scavengers. *Ind. Eng. Chem. Res.* **2011,** *50*, 735-740. https://doi.org/10.1021/ie101985v

(9) Madsen, H. T.; Søgaard, E. G. Use of ESI-MS to Determine Reaction Pathway for Hydrogen Sulphide Scavenging With 1,3,5-Tri-(2-Hydroxyethyl)-Hexahydro-*S*-Triazine. *Eur. J. Mass Spectrom.* **2012,** *18*, 377-383. https://doi.org/10.1255/ejms.1192

(10) Taylor, G. N.; Prince, P.; Matherly, R.; Ponnapati, R.; Tompkins, R.; Vaithilingam, P. Identification of the Molecular Species Responsible for the Initiation of Amorphous Dithiazine Formation in Laboratory Studies of 1,3,5-Tris(Hydroxyethyl)-Hexahydro-S-Triazine as a Hydrogen Sulfide Scavenger. *Ind. Eng. Chem. Res*. **2012,** *51*, 11613-11617. https://doi.org/10.1021/ie301288t

(11) Madsen, H. T.; Søgaard, E. G. Fouling Formation During Hydrogen Sulfide Scavenging with 1,3,5-Tri-(Hydroxyethyl)-Hexahydro-S-Triazine. *Pet. Sci. Technol.* **2014,** *32*, 2230-2238. https://doi.org/10.1080/10916466.2013.783066

(12) Fiorot, R. G.; Carneiro, J. W. de M. The Mechanism for H_2S Scavenging by 1,3,5-Hexahydrotriazines Explored by DFT. *Tetrahedron* **2020,** *76*, 131112. https://doi.org/10.1016/j.tet.2020.131112

(13) Montesantos, N.; Fini, M. N.; Muff, J.; Maschietti, M. Proof of Concept of Hydrothermal Oxidation for Treatment of Triazine-Based Spent and Unspent H_2S Scavengers from Offshore Oil and Gas Production. *Chem. Eng. J.* **2022,** *427*, 131020. https://doi.org/10.1016/j.cej.2021.131020

(14) Lioliou, M. G.; Jenssen, C. B.; Øvsthus, K.; Brurås, A. M.; Aasen, Ø. L. Design Principles for H_2S Scavenger Injection Systems. Presented at the Oilfield Chemistry Symposium, Geilo, Norway, March 2018.

(15) Perez Pineiro, R.; Peeples, C. A.; Hendry, J.; Hoshowski, J.; Hanna, G.; Jenkins, A. Raman and DFT Study of the H_2S Scavenger Reaction of HET-TRZ Under Simulated Contactor Tower Conditions. *Ind. Eng. Chem. Res*. **2021,** *60*, 5394-5402. https://doi.org/10.1021/acs.iecr.1c00852

(16) Perez Pineiro, R.; Cruz-Perez, D.; Hoshowski, J.; Zhang, H.; Hendry, J. H_2S Scavenger Tower Operational Efficiency Achieved Through Onsite Compositional Analysis. Volume 1. In *Proceedings of the Corrosion Conference and Expo 2018.* NACE International: Houston, TX, 2018; p. 5336.

(17) Johansen, L. N.; Kloster, L.; Andreasen, A.; Kucheryavskiy, S.; Nielsen, R. P.; Maschietti, M. Raman Spectroscopy for Monitoring Aqueous Phase Hydrogen Sulfide Scavenging Reactions with Triazine: A Feasibility Study. *Chem. Eng. Trans*. **2019,** *74*, 541-546. https://doi.org/10.3303/CET1974091

(18) OndaVia, Inc., Chemical Identification with Raman Spectroscopy: Part 2. https://www.ondavia.com/node/99 (Accessed December 2020)

(19) Wold, S.; Sjöström, M.; Eriksson, L. PLS-Regression: A Basic Tool of Chemometrics. *Chemom. Intell. Lab. Syst*. **2001,** *58*, 109-130. https://doi.org/10.1016/S0169-7439(01)00155-1

(20) Eilers, P. H. C. A Perfect Smoother. *Anal. Chem*. **2003,** *75*, 3631-3636. https://doi.org/10.1021/ac034173t

(21) R Development Core Team and the R Foundation. The R project for Statistical Computing. https://www.R-project.org (accessed May 2021)

(22) Kucheryavskiy, S. mdatools - R Package for Chemometrics. *Chemom. Intell. Lab. Syst*. **2020,** *198*, 103937. https://doi.org/10.1016/j.chemolab.2020.103937

(23) Beleites, C.; Sergo, V. (0.100.0). *hyperSpec: A Package to Handle Hyperspectral Data Sets in R*. R package version 0.100.0. https://github.com/cbeleites/hyperSpec (accessed May 2021)

(24) Rayer, A. V.; Sumon, K. Z.; Jaffari, L.; Henni, A. Dissociation Constants (pK_a) of Tertiary and Cyclic Amines: Structural and Temperature Dependences. *J. Chem. Eng. Data* **2014,** *59*, 3805-3813. https://doi.org/10.1021/je500680q

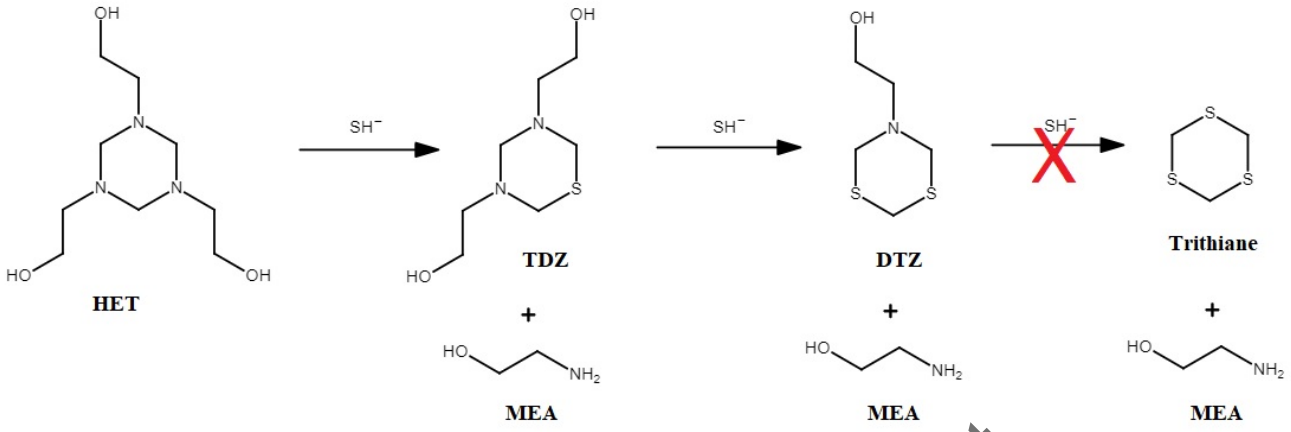

431

432 **Figure 1.** Simplified reaction scheme reporting the stoichiometry of the aqueous phase H_2S scavenging

433 reactions using MEA-triazine (HET).

434

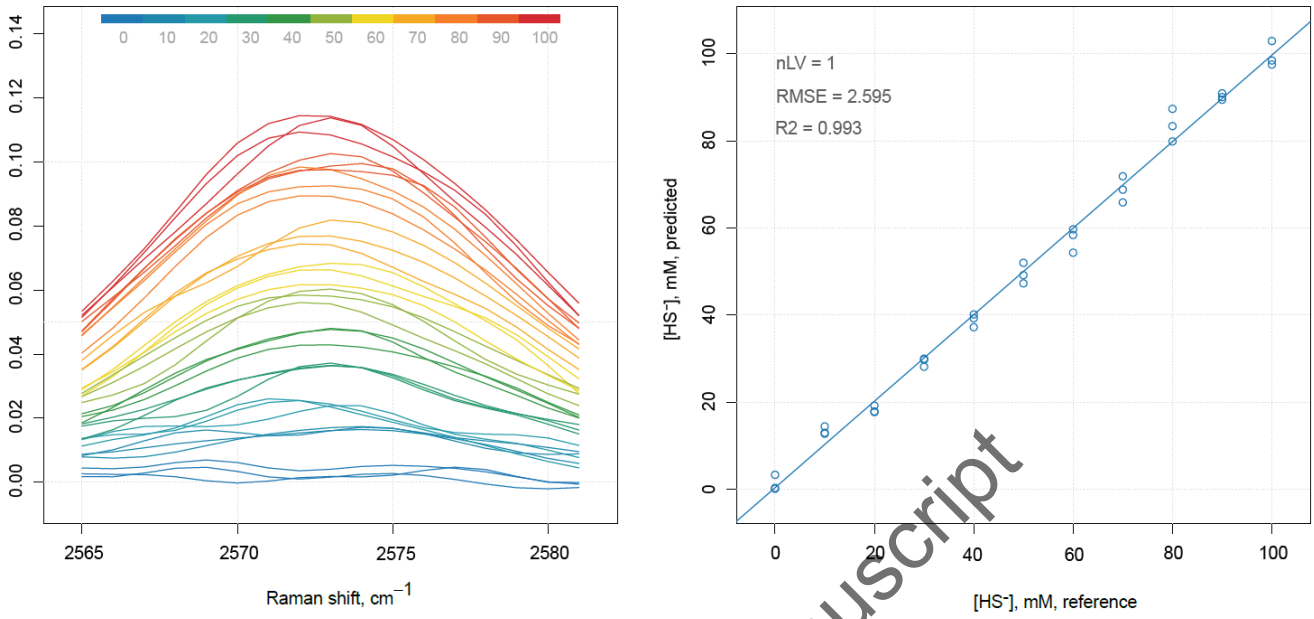

435

436 **Figure 2.** Calibration of the PLS regression model. The left plot shows the preprocessed and truncated

437 Raman spectra used for the calibration of the model (the lines are color grouped according to the

438 concentration of HS^-) with the ordinate axis representing the peak intensity. The color legend shows the

439 concentrations of HS^- expressed in mM. The right plot shows predicted vs. measured values and the

440 main performance statistics for the final PLSR model (cross-validated results).

441

442

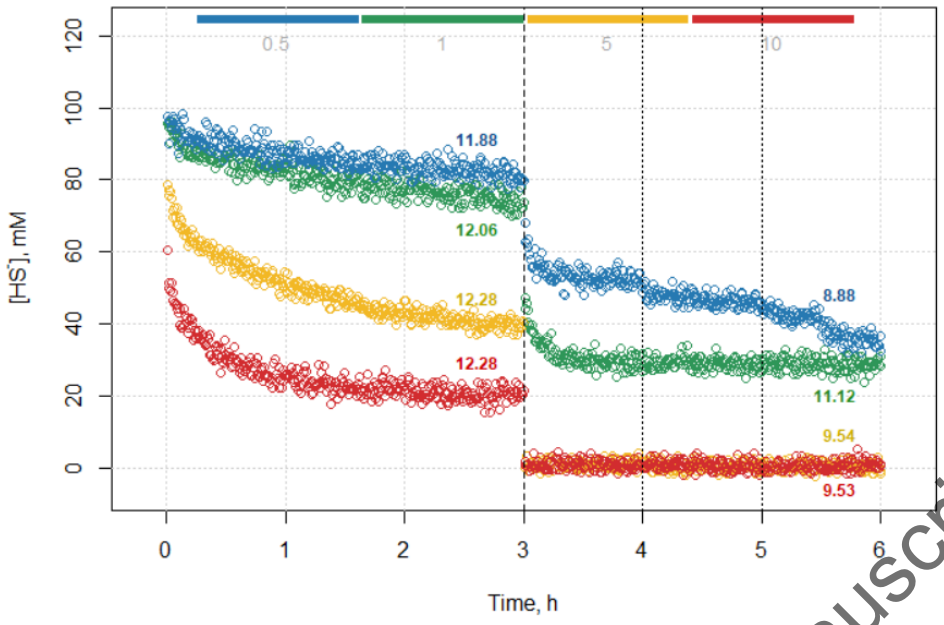

443

444 **Figure 3.** Effect of the initial concentration of HET on the conversion of HS^- for $pH_0 = 9$. The colors are

445 associated with different values of the initial concentration ratio HET/HS^-: blue 0.5; green 1; yellow 5;

446 red 10. The numbers on the plot report the measured pH values after 3 h (before the first acidification)

447 and after 6 h. Vertical dashed line: re-acidification after 3 hours (all samples). Dotted lines: additional

448 re-acidifications (only for the initial concentration ratio HET/HS^- of 0.5).

449

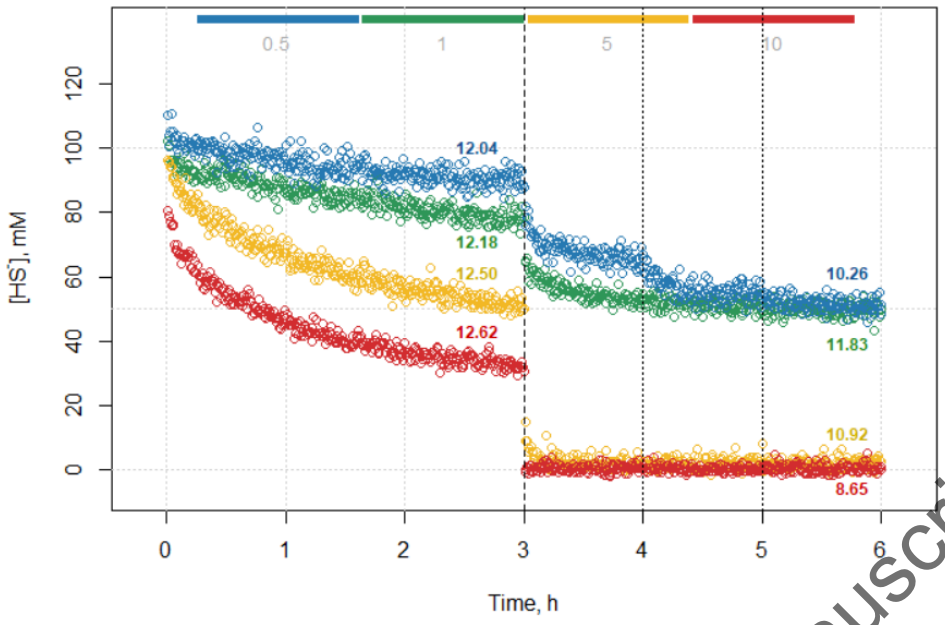

450

451 **Figure 4**. Effect of the initial concentration of HET on the conversion of HS^- for $pH_0 = 10$. The colors
452 are associated with different values of the initial concentration ratio HET/HS^-: blue 0.5; green 1; yellow
453 5; red 10. The numbers on the plot report the measured pH values after 3 h (before the first acidification)
454 and after 6 h. Vertical dashed line: re-acidification after 3 hours (all samples). Dotted lines: additional
455 re-acidifications (only for the initial concentration ratio HET/HS^- of 0.5).

456

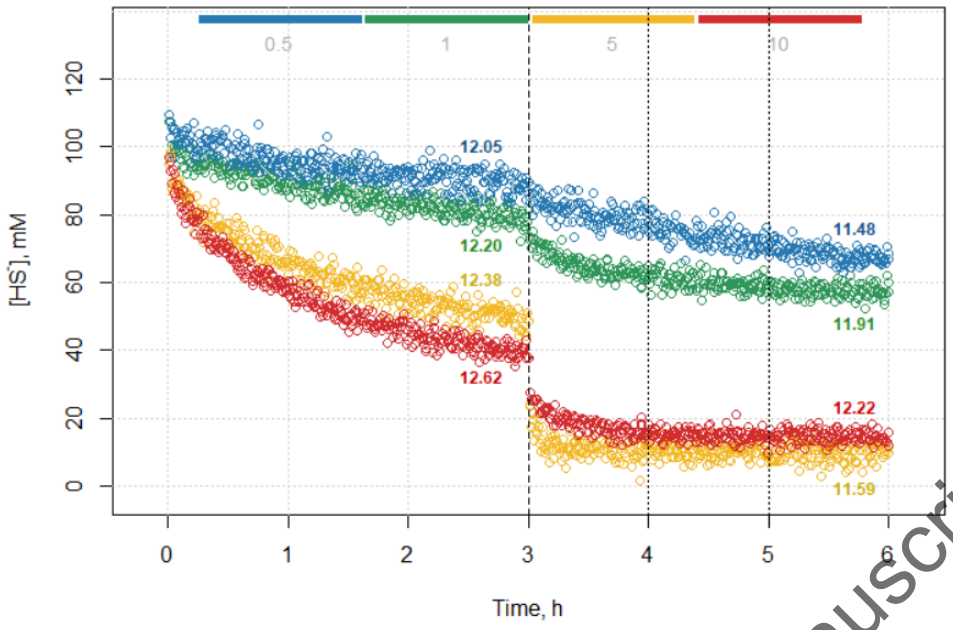

457

458 **Figure 5.** Effect of the initial concentration of HET on the conversion of HS^- for $pH_0 = 11$. The colors

459 are associated with different values of the initial concentration ratio HET/HS^-: blue 0.5; green 1; yellow

460 5; red 10. The numbers on the plot report the measured pH values after 3 h (before the first acidification)

461 and after 6 h. Vertical dashed line: re-acidification after 3 hours (all samples). Dotted lines: additional

462 re-acidifications (only for the initial concentration ratio HET/HS^- of 0.5).

463

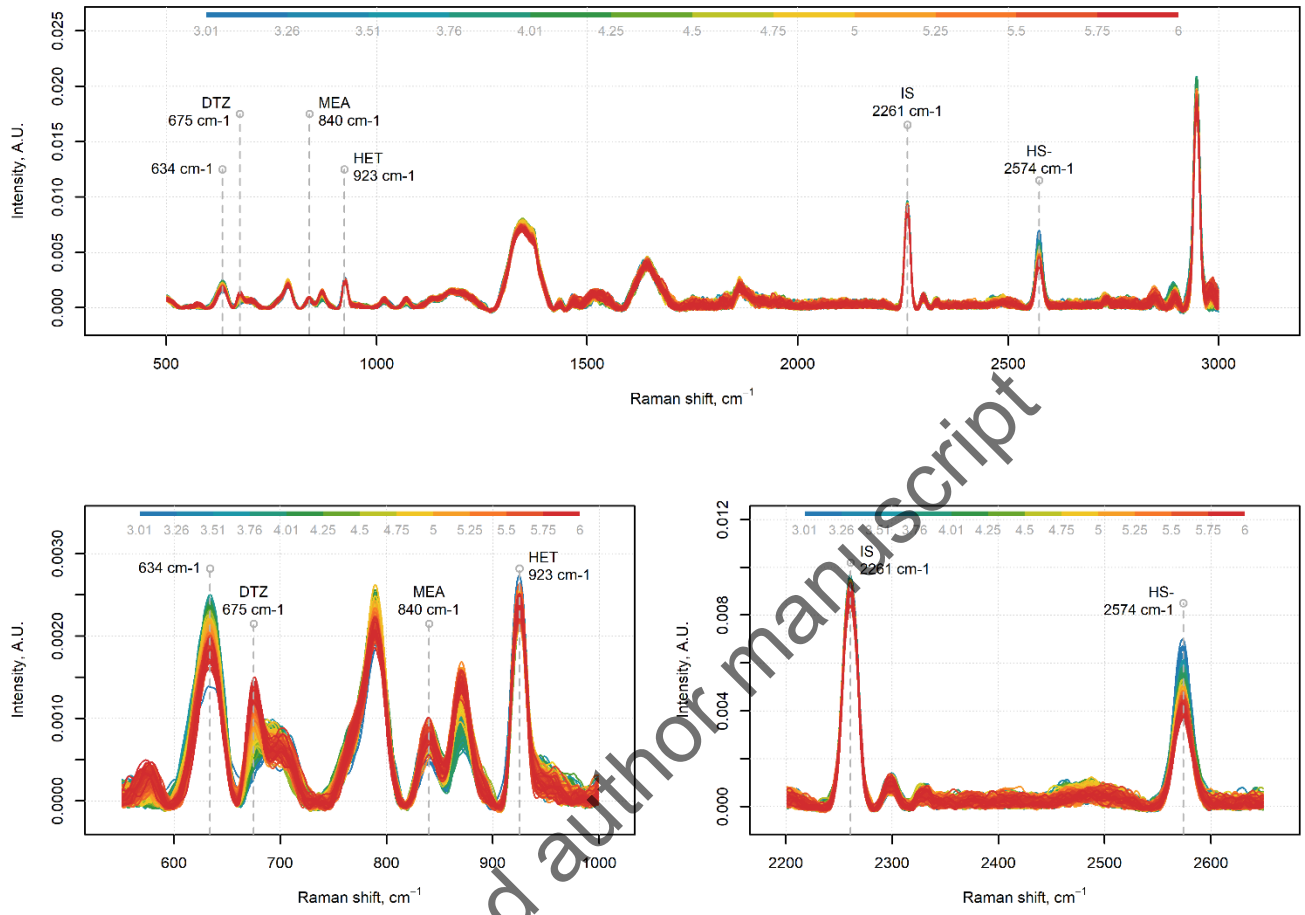

464

465 **Figure 6.** Raman spectra of the aqueous phase reaction between HS^- and HET at pH_0 = 9 and initial

466 concentration ratio 0.5, from t = 3 h until t = 6 h (after acidification), colored by reacting time. The color

467 legend shows the reaction times in hours. Selected peaks for HET, DTZ and MEA, as well as peaks for

468 HS^- and internal standard (IS), are indicated with gray dashed lines.

469

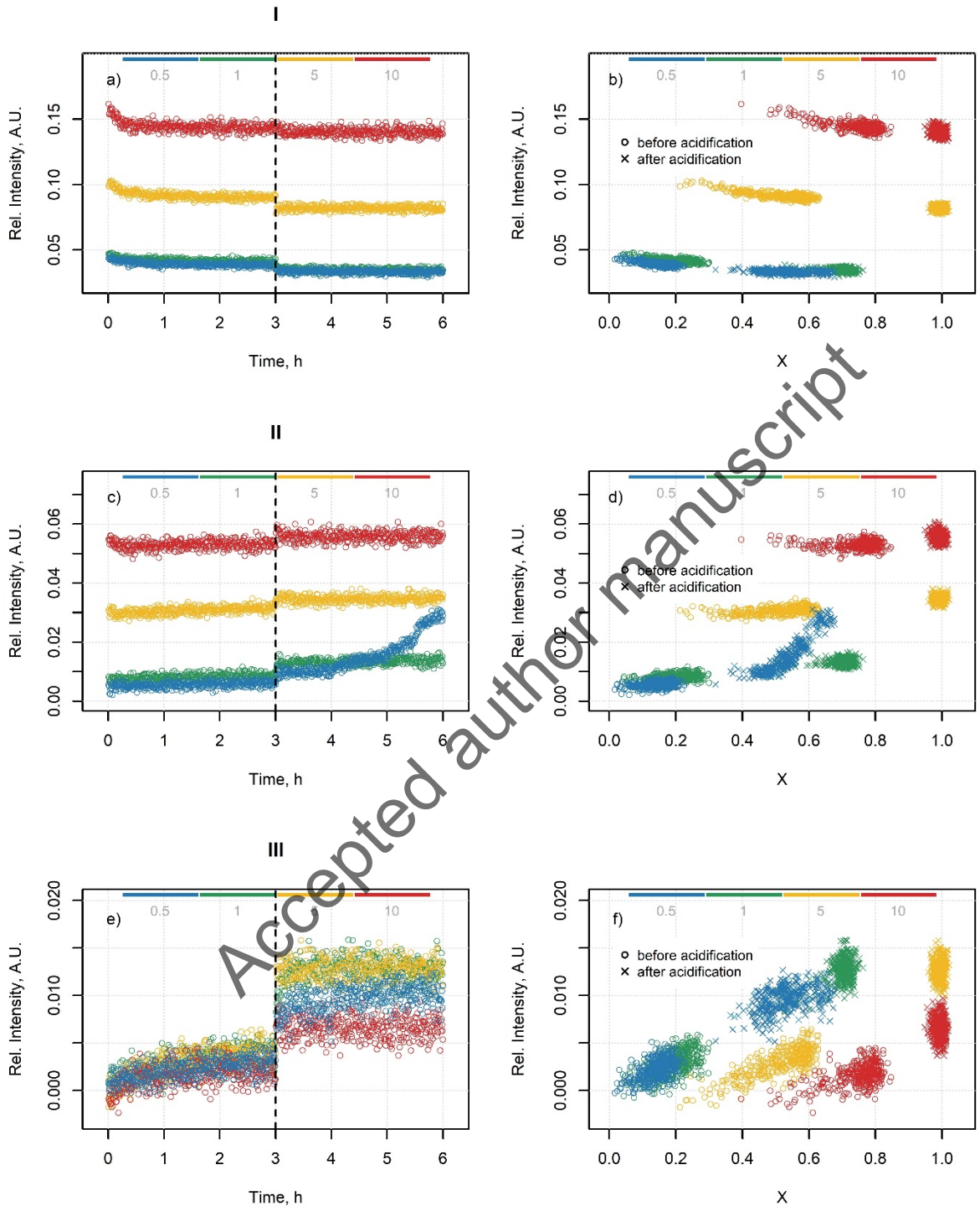

470

471 **Figure 7.** Relative intensity of peaks for executions at $pH_0 = 9$ as a function of time (a, c, e) and as a

472 function of HS^- fractional conversion (b, d, f) for HET (I), DTZ (II) and MEA (III).

473 **Table 1.** Values of fractional conversion of HS^- (X) before acid injection (1 h, 3 h) and after acid injection

474 (6 h) with corresponding standard deviation (SD) values.

		X %		
$[HET]_0/[HS^-]_0$	**pH_0**	**1 h**	**3 h**	**6 h**
0.5	9	11.6 ± 5.4	21.8 ± 2.5	63.2 ± 0.2
0.5	10	6.0 ± 3.1	12.7 ± 1.1	50.9 ± 1.0
0.5	11	5.8 ± 1.4	12.5 ± 3.3	38.9 ± 8.5
1	9	17.3 ± 1.3	28.3 ± 3.0	72.4 ± 1.3
1	10	11.4 ± 1.5	20.9 ± 0.6	48.7 ± 1.9
1	11	7.8 ± 4.5	17.2 ± 2.0	42.3 ± 0.5
5	9	47.5 ± 4.7	59.7 ± 0.4	99.0 ± 1.4
5	10	31.9 ± 0.7	49.9 ± 0.0	99.8 ± 0.3
5	11	30.7 ± 9.7	45.9 ± 7.8	79.5 ± 11.5
10	9	71.8 ± 2.8	79.9 ± 2.1	99.0 ± 0.4
10	10	53.1 ± 2.0	68.7 ± 1.1	99.6 ± 0.5
10	11	41.4 ± 2.4	63.7 ± 2.1	86.1 ± 2.5

475

476